Solid State Ionics 314 (2018) 41–45

Contents lists available at ScienceDirect

Solid State Ionics

journal homepage: www.elsevier.com/locate/ssi

Novel silicon–tungsten oxide–carbon composite as advanced negative electrode for lithium-ion batteries

Hyun-seung Kim[a], Jongjung Kim[a], Jae Gil Lee[a], Ji Heon Ryu[b], Jaekwang Kim[c], Seung M. Oh[a,*], Songhun Yoon[c,*]

[a] Chemical and Biological Engineering and WCU Program of Chemical Convergence for Energy & Environment (C2E2), Seoul National University, Seoul 151-744, Republic of Korea
[b] Graduate School of Knowledge-based Technology and Energy, Korea Polytechnic University, 2121 Jeongwang-dong, Siheung-si, Gyeonggi-do 429-793, Republic of Korea
[c] School of Integrative Engineering, Chung-Ang University, 221, Heukseok-Dong, Dongjak-Gu, Seoul 156-756, Republic of Korea

ARTICLE INFO

Keywords:
Alloying reaction
Negative electrode
Conversion reaction
Tungsten oxide
Chemical synthesis

ABSTRACT

A cheap Si powder byproduct from solar cell production was applied as a negative electrode for lithium-ion batteries. To improve the cycle and rate performances, the as-obtained Si powder was composited with tungsten oxide and coated with carbon, in sequence. After preparing the composite material, its electrochemical performance is evaluated, which exhibits a high reversible capacity of 975 mA h g^{-1} with improved cycleability. Especially, the rate capability is significantly improved to 390 mA h g^{-1} under 1000 mA g^{-1} applied current. This advanced electrochemical performance is attributed to the matrix effect of the formed Li_2O and W metal with carbon coating, as identified using ex-situ X-ray diffraction experiments, and associated with the low polarization resistance observed in the galvanostatic charge intermittent technique.

1. Introduction

Li-ion batteries (LIBs), as highly promising energy storage systems, have been applied to mobile devices and electric vehicles [1–7]. To extend the available driving range of electric vehicles, LIBs must have high volumetric energy and power densities because their occupied volume is strongly limited in electric vehicle applications [8]. For this purpose, improvements in the gravimetric and volumetric capacities of electrode materials are necessary. As a material with a high gravimetric capacity, Si has been proposed as a promising negative electrode because it has a high theoretical capacity and low working voltage below 0.4 V (vs. Li/Li^+) [9–13]. Unfortunately, Si negative electrodes suffer dramatic volumetric stresses of ~400% during lithiation and de-lithiation [9,14,15]. A more severe problem is the facile degradation of the electrode structure caused by electrical contact loss upon de-lithiation of the Si [9]. To alleviate electrode failure from volumetric change-induced mechanical cracking and dead particle generation, nano-sized Si, having a large free volume, has been recommended to reduce mechanical stress [16–18]. Moreover, the nano structure of Si is applied to enhance the cycleability of Si, such as nanotubes, nanowires [19,20]. However, this approach entails several difficulties, such as inhomogeneous slurry mixing, increased conducting agent for sufficient electrical contact, and possible internal electric short-circuiting from weakly attached nanoparticles. Furthermore, instability of solid electrolyte interphase on silicon-based negative electrodes during cycle and high temperature storage is emerged as problematic feature for practical application [21,22]. From a practical perspective, therefore, microscale Si is appropriate, although the possibility of particle cracking during charge–discharge cycling remains high [9,18]. From the literature, the trapping of Li^+ at Si particles is considered the dominant failure mode with microscale Si negative electrodes [18]. By introducing a buffer matrix or partially oxidized Si, increases in the capacity retention of electrodes have been reported [23–25].

Possible candidates for high-volumetric-capacity LIB negative electrodes also include oxides of heavy transition metals (e.g., Mo and W). W oxide negative electrodes have exhibited very high gravimetric capacities reaching 748 mA h g^{-1}. Because of the high oxidation number of W in oxides (~6 +), approximately 3 mol Li_2O per 1 mol W^0 can be produced during the charging reaction, indicating a high reversible capacity [26]. A high volumetric capacity of ~2000 mA h cm^{-3} was previously reported because of the intrinsically high material density of WO_3 at 7.61 g cm^{-3}. Because W oxides have higher-voltage conversion reactions than Si does, W and Li_2O phases can act as conductive networks and buffer phases for the relaxation of mechanical stress by the lithiation of Si [21–24]. To improve the cycle and rate capability of Si negative electrodes, reduced metal oxides must remain inactive at the

* Corresponding authors.
E-mail addresses: seungoh@snu.ac.kr (S.M. Oh), yoonshun@cau.ac.kr (S. Yoon).

https://doi.org/10.1016/j.ssi.2017.11.013
Received 8 September 2017; Received in revised form 13 November 2017; Accepted 20 November 2017

lithiation voltage of Si; the as-formed W metal can therefore enhance electrical conductivity [27–30].

Herein, a silicon–tungsten oxide–carbon (STC) composite is prepared as a novel negative electrode for LIBs. By incorporating W oxide into the Si negative electrode and coating the negative electrode with C, the cycleability and rate capability of the negative electrode are expected to improve because of the generation of nanoscale W metal and a buffer matrix of Li_2O. Subsequently, microscale Si and STC electrodes are compared. Finally, the rate capability is compared for these electrodes and the polarization is examined by the galvanostatic intermittent titration technique (GITT).

2. Experimental section

2.1. Synthesis of Si composite

Si powder was obtained from a conventional reactor for the preparation of polysilicon, which can be used for producing Si solar cell wafers. The Si powder was mixed with Pluronic P-123 surfactant, phosphotungstic acid ($H_3PW_{12}O_{40}$), and sucrose in an ethanol solvent. After stirring for 2 h, the solvent was evaporated using a rotary evaporator and then heat-treated at 600 °C for 4 h under a 5% H_2/Ar mixed gas for obtaining a better reducing atmosphere. After heat-treatment, the weight ratios of Si, WO_3, and C were estimated at 1/1/0.14 using thermal gravimetric analysis (TGA).

2.2. Electrochemical characterization

A 2032-type coin cell was employed for testing the electrochemical performances of WO_3, the synthesized Si composite, and the bare Si material (Alfa Aesar, APS 1–5 μm, 99.9% (metals basis)). The composite electrode was prepared by casting the slurry of Si–WO_3–C composite powders, Si, or WO_3; Super P; and poly(acrylic acid) Li salt (LiPAA) in a 7:2:1 wt. ratio on Cu foil. The weigh loading of electrode was 0.8 mg cm^{-2}. The electrodes were dried at 120 °C in a vacuum atmosphere overnight. After drying the electrode, its electrochemical performance was tested. Li foil was used as the counter and reference electrodes. 1.3 M $LiPF_6$ in fluoroethylene carbonate (FEC):ethyl methyl carbonate (EMC):diethyl carbonate (DEC) (3:2:5 = v/v) was used for the electrolyte solution. A porous polypropylene–polyethylene–polypropylene (PP–PE–PP) separator was used to prevent mechanical shortage. In the first (formation) cycle, a galvanostatic charge–discharge experiment was conducted in the potential range of 0.05–1.5 V (vs. Li/Li^+). After formation, the potential window for cycling was set as 0.07–1.5 V (vs. Li/Li^+).

2.3. Ex-situ X-ray diffraction (XRD) spectroscopy

Ex-situ XRD patterns of the lithiated/de-lithiate Si–WO_3–C composite electrode (voltage cut-off: 50 mV) comprising Si–WO_3–C composite, Super P, and LiPAA (7:2:1 wt. ratio) were collected by a DMAX2500-PC (Rigaku Co.) diffractometer using Cu-Kα radiation (1.5406 Å).

2.4. FE-SEM imaging

The synthesized particle morphology was observed by field-emission scanning electron microscopy (FE-SEM, JEOL JSM-6700F).

2.5. Galvanostatic intermittent titration technique (GITT) and polarization measurement for two electrodes

A 10-min galvanostatic step and 20-min rest period was applied to analyze the polarization of the two electrodes within the potential range of 0.05–1.5 V (vs. Li/Li^+). The polarization of each quasi-open-circuit voltage was calculated from the difference between the closed-circuit voltage and quasi-open-circuit voltage in transient voltage profiles.

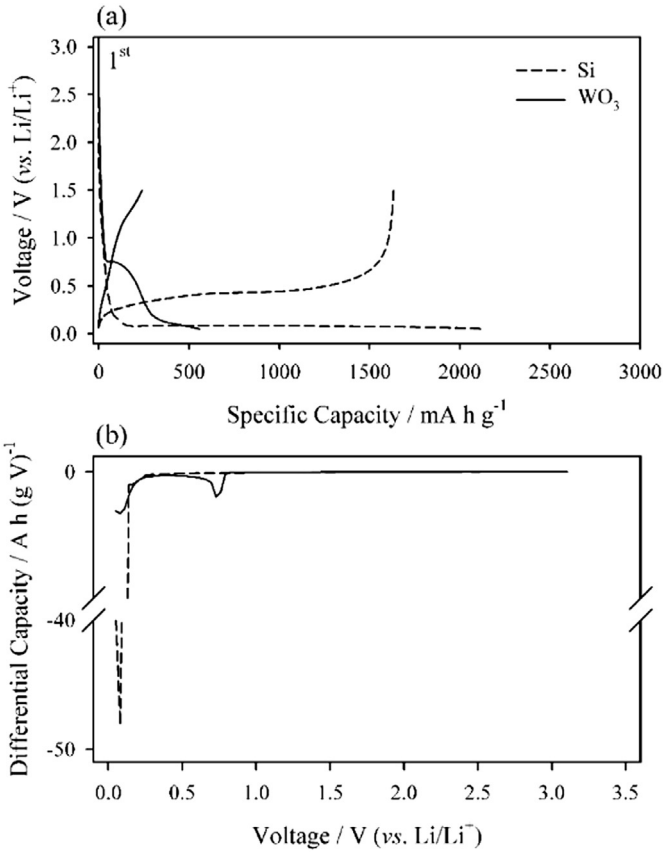

Fig. 1. (a); Initial voltage profiles of Si and WO_3. (b); lithiation differential capacity plot of Si and WO_3 at 50 mA g^{-1} with voltage cut-off of 0.05 to 1.5 V (vs. Li/Li^+).

3. Results and discussion

To identify the matrix role of WO_3 and relevant charging mechanisms, bulk WO_3 and as-obtained Si powder were applied as negative electrodes in LIBs. The morphology of the used Si powder and as-prepared WO_3 material was investigated using FE-SEM and XRD, as displayed in Figs. S1 and S2. In Fig. S1, the tungsten oxide which was prepared without Si and carbon was displayed. As seen, bulk powder was obtained and its crystal structure was identified using XRD as shown in Fig. 1b. Typical WO_3 with PDF #880550 was obtained. The as-obtained Si powder comprised several 10-μm-sized secondary particles with sub-micrometer Si primary particles, as shown in Fig. S2. Because gas-phase precursors such as SiH_4 are employed in polysilicon production, the obtained Si powder as a side product has spherical primary particles. Meanwhile, the prepared WO_3 has particles crushed from the monolithic structure of the bulk material.

Fig. 1 presents the first lithiation and de-lithiation voltage profiles of the WO_3 and Si negative electrode cells. As seen, it is confirmed that WO_3 is lithiated by the conversion reaction before reaching the lithiation voltage of Si, while showing lithiation and de-lithiation capacities of 550 mA h g^{-1} and 215 mA h g^{-1}, respectively, at the voltage cut-off of 1.5 V (vs. Li/Li^+) with a 39% initial efficiency. The Si powder shows lithiation and de-lithiation capacities of 2015 and 1620 mA h g^{-1}, respectively. From the differential capacity plot in Fig. 1b, the lithiation voltages of WO_3 and Si can be observed more clearly, confirming that the initial lithiation voltage of WO_3 is higher than that of Si. This indicates that a buffer matrix of the Li_2O phase and a conductive matrix of metallic W can be generated in the WO_3 negative electrode.

Fig. 2a displays an FE-SEM image of the STC material. As seen, sub-micrometer primary particles form secondary particles of large sizes exceeding 10 μm, which is a highly suitable morphology for the electrode coating process, as it decreases the consumption of *N*-methyl-2-